Geochimica Brasiliensis, **2**(2):185-199, 1988

THE SÃO JOSÉ DO RIO PARDO MANGERITIC-GRANITIC SUITE, SOUTHEASTERN BRAZIL

M.C. Campos Neto[1], M.C.H. Figueiredo[1], V.A. Janasi[1], M.A.S. Basei[1], B.J. Fryer[2]

1. Instituto de Geociências, Universidade de São Paulo. Caixa Postal 20.899, 01498 São Paulo, Brasil
2. Department of Earth Sciences, Memorial University of Newfondland, St. John's AlB 3X5, Canada

ABSTRACT

In the São José do Rio Pardo region, São Paulo and Minas Gerais States, occur some intrusive, folded, tabular bodies of mangerites associated with hornblende granitoids. The country rocks correspond to a complex association of gneisses and migmatites, locally with granulite facies assemblages. Both the mangerites and hornblende granitoids present a tectonic foliation with mineral flattening and stretching.

Petrographically the mangeritic rocks are mainly dark green quartz mangerites with mesoperthite, plagioclase, quartz, hypersthene, clinopyroxene and variable amounts of hornblende, with zircon as conspicuous acessory. The pink hornblende granitoids are mainly granite s.s. exhibiting higher quartz and amphibole contents and lacking pyroxenes. Hololeucocratic alkali feldspar granites are locally associated to these hornblende granites. The textures of the mangerites and granites almost always show an important metamorphic overprinting, with relictic mesoperthite and pyroxene crystal into a granoblastic matrix.

The mangeritic-granitic suite is characterized by relatively high Fe/(Fe + Mg), K and HFS elements and low Ca contents, being comparable to typical anorogenic mangeritic-granitic suites from Scandinavia and North America.

The Rb/Sr data indicate a Late Proterozoic metamorphic isotopic rehomogenization (930 Ma, Ro = 0.706). Geological evidence suggest that the intrusive age could be Middle Proterozoic, which is reinforced by another Rb-Sr value of about 1300 Ma.

RESUMO

Mangeritos associados a hornblenda granitos ocorrem, em corpos intrusivos tabulares e dobrados, na região de São José do Rio Pardo (SP-MG). Encaixam-se em uma complexa associação gnáissico-migmatítica, localmente na fácies granulito. Uma foliação tectônica com achatamento e/ou estiramento mineral encontra-se impressa nessas rochas.

Petrograficamente dominam quartzo mangeritos verde-acinzentados a mesopertitas, plagioclásio, quartzo, hiperstênio, clinopiroxênio e hornblenda, com zircão como acessório freqüente. Os hornblenda granitóides róseos são granitos s.s., ricos em quartzo e anfibólio e, localmente associam-se a microclina granitos hololeucocráticos. A textura destas rochas é metamórfica, com mesopertitas e cristais de piroxênio, reliquiares, em uma matriz granoblástica.

A suite mangerito-granítica caracteriza-se por altos conteúdos relativos em K, Zr, Nb e Y e altos valores na razão Fe(Fe + Mg); contrapondo-se a baixos valores em Ca. É comparável com as suites mangerito-graníticas anorogênicas da Escandinávia e América do Norte.

Os dados de Rb-Sr indicam um evento de rehomogeneização isotópica no Proterozóico Superior (930 Ma, Ro = 0,706). Evidências geológicas sugerem que a idade de intrusão deveria ser no Proterozóico Médio, o que é reforçado por outro valor Rb-Sr de cerca de 1300 Ma.

INTRODUCTION

The first descriptions of hypersthene-bearing rocks in northeastern São Paulo-southwestern Minas Gerais states are due to Ebert (1968) who recognized both ortho- and para- "charnockitic" rocks and considered them as small bodies dehydrated by mylonitization previously to the main regional metamorphic event.

Oliveira (1973) and Oliveira & Alves (1974) studied the occurrences near São José do Rio Pardo and Caconde, mapping a "granulitic association" including basic to acid "calc-alkalic" hypersthene granulites and hololeucocratic granitic gneisses with flaser textures. The granulites were considered to correspond to dehydrated residua of an anatectic process.

Further regional (Cavalcante *et al.*, 1979) and semi-detailed geological mapping (Oliveira *et al.*, 1983, 1984; Campos Neto & Figueiredo, 1985) showed that the charnockitic rocks and associated granitic gneisses form two roughly parallel batholithic bodies elongated in the NW-SE to NNW-SSE directions, each of them about 100 km long. They are intruded by the Cretaceous alkaline Poços de Caldas massif and covered, to the west, by the Phanerozoic units of the Paraná Basin (Fig. 1).

Campos Neto & Figueiredo (1985) firstly recognized the plutonic character of the charnockitic-granitic association, as well as the dominantly quartz-poor nature of the hypersthene-bearing rocks, thus classified as mangerites. The associated pink granitoids with flaser structure, generally corresponding to hornblende granites with locally abundant hololeucocratic alkali feldspar granites, were showed to locally grade into the mangerites, so suggesting a cogenetic relationship among these rock types.

Isotopic data have been published by Oliveira (1973) — K-Ar and model Rb-Sr ages — and by Oliveira *et al.* (1986) — Rb-Sr isochrons and zircon U-Pb data — defining Late Proterozoic ages with all the employed methods.

This work presents new field, petrographic, chemical and isotopic data on the São José do Rio Pardo lithologies and proposes a new interpretation to their signification in the regional geological context, based upon their structural relationships and close similarities to anorogenic mangeritic-granitic associations found elsewhere.

REGIONAL GEOLOGY

The region under investigation is characterized by larger thrust nappes (Socorro and Guaxupé) juxtaposing infracrustal high-grade terrains — The Alto Rio Grande Belt (Fig. 1).

The Alto Rio Grande Belt (Hasui & Oliveira, 1984) consists of a supracrustal sequence ranging from a volcanosedimentary rif-type unit to a quartzitic-carbonatic platform at the southern border of the São Francisco Craton (Vasconcellos, 1988). It is structured as refolded anticlinal nappes of the second folding phase, with northward vergence, having low- to medium grade Barrovian-type metamorphism increasing southwards (Trow *et al.*, 1983; Vasconcellos, 1988). This belt appears to correspond to a Middle Proterozoic unit with an Archean-Early Proterozoic basement.

The Socorro and Guaxupé thrust nappes (Campos Neto, 1985) are complex crustal flakes with northwestward transported high-grade metamorphic belts, consisting of a lower thrust emplaced during the late stages of the Middle Proterozoic superposed by a Late Proterozoic thrust. The first thrust engages a high-pressure metamorphic association of granulites, gneissic granitoids and migmatites, while the second represents a low-pressure association of granitic-migmatitic terrains, with migmatized metasediments at the top of the allochthonous structure. The São José do Rio Pardo mangeritic-granitic suite occurs at the front of this second structure (Fig. 1). These thrust nappes represent allocthonous terranes in relation to the Alto Rio Grande Belt and the reworked marginal zone of the São Francisco Craton.

LOCAL GEOLOGY

In the studied region, the mangeritic-granitic suite occurs into a dominantly orthogneissic-migmatitic complex, which is piled up by thrust zones over a high-grade supracrustal sequence cropping out towards northeast (Fig. 2).

The supracrustal sequence is locally dominated by strongly migmatized banded gneisses (hornblende or garnet-biotite-bearing) with an intermediate unit of quartzites and quartz-rich gneisses. Granulite facies assemblages are found in gneissic rocks near the south-southwestern tectonic limit of this complex.

In the allochthonous orthogneissic-migmatitic complex several types of granitic-gneissic rocks occur, their mutual relations being frequently masked by strong migmatisation. Besides the mangeritic-granitic association, three major units can be recognized: stromatic migmatites, porphyroclastic granitoids and younger granitoids.

The stromatic migmatites comprise a complex association with gneissic mesosomes (in the sense of Johannes & Gupta, 1982) of varied composition. The dark-grey mesosomes are dioritic-tonalitic and hornblende-biotite (± clinopyroxene)-bearing. They often show centimetric medium to coarse grained, foliated, white leucosomes of throndhjemitic composition, surrounded by irregular mafic-rich melanosomes. Grey or pinkish mesosomes have granitic-granodioritic composition and are biotite (± hornblende)-bearing. They have medium to coarse grained pink granitic leucosomes, which also occur in the dark-grey mesosomes where they are later than the trondhjemitic leucosomes.

The porphyroclastic granitoids form irregular bodies sometimes of batholitic dimensions. They consist of gneissic granitoids with pink augen alkali feldspar megacrysts (2 cm on average but locally up to 10 cm) in a biotite-hornblende (± clinopyroxene)-bearing grey matrix. Decimetric to metric enclaves of dioritic-monzodioritic gneisses and calc-silicate rocks (with garnet, diopside and scapolite) are common. Lenticular bodies (up to 3 km long) of kinzigitic gneisses (with quartz, sillimanite, garnet, biotite, cordierite, spinel ± feldspars) locally occur among these porphyroclastic granitoids.

The younger intrusive rocks form small bodies of isotropic to slightly foliated equigranular pink biotite granites, often with nebulitic structures and are probably related with the late anatectic event.

STRUCTURAL GEOLOGY

Almost all rock types occurring in the region are gneissic and highly deformed, presenting a predominantly flat lying and tabular shape.

An originally sub-horizontal foliation is generally parallel to the lithological contacts. This foliation is a primary tectonic structure in the orthogneissic-migmatitic complex acting with different intensities by pure or ductile shearing under high-grade metamorphic conditions.

The foliation produced by pure shearing is strongly planar with platy quartz defining a thin banding by metamorphic segregation, sometimes having a main mineral stretching direction associated to dissolution processes in pressure shadow zones. When formed by shearing the foliation has a dominant stretching direction producing an intense linear to plane-linear structure associated to monomineralic rods, pinch and swell and boudinage structures and sheath folds.

The planar structure is parallel to the axial planes of similar to subclass 1C folds of the syncinematic neosomes. The main statistical orientation of the mineral stretching lineation is S40E/10° indicating a transport in the NW-SE direction.

The foliation is subjected to an inverse folding of the subclass 1C with a new main orientation NW-SE slightly dipping towards SW. These folds with northeastward vergence have centimetric to kilometric dimensions (Fig. 3) reaching

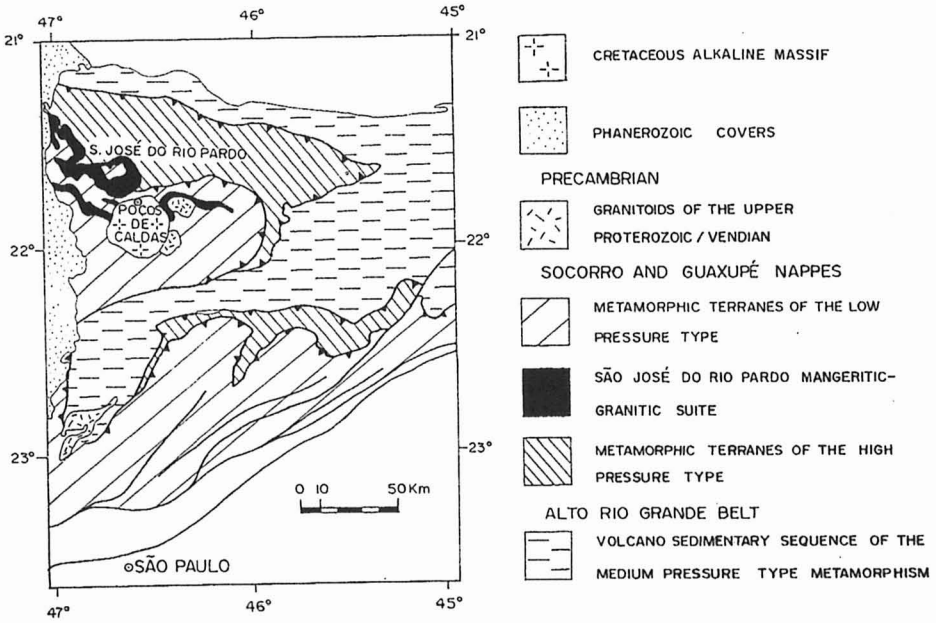

Figure 1 — Regional geological map.

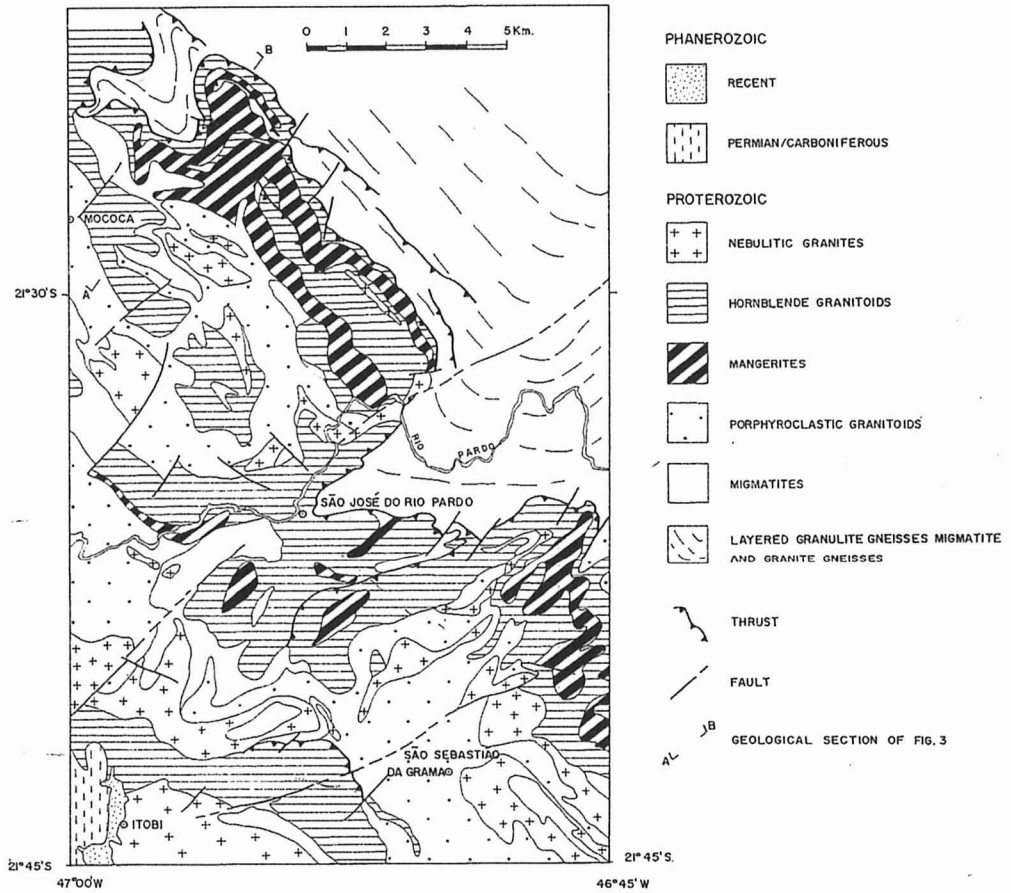

Figure 2 — Geological map of the São José do Rio Pardo region.

3.5 km of wavelenght with an estimated amplitude of 3 km. This folding phase occurred under amphibolite facies conditions with biotite and/or hornblende recrystallization in local axial plane foliations. Granitic injections use to occur along the axial planes of the folds, sometimes associated to ductile shearing belts.

The tectonic piling of the orthogneissic-migmatitic complex over the high-grade supracrustal sequence is made by a northeastward thrusting which produces mylonites and blastomylonites under low-grade metamorphic conditions (chlorite-bearing).

Generally cylindrical and isopach open folds

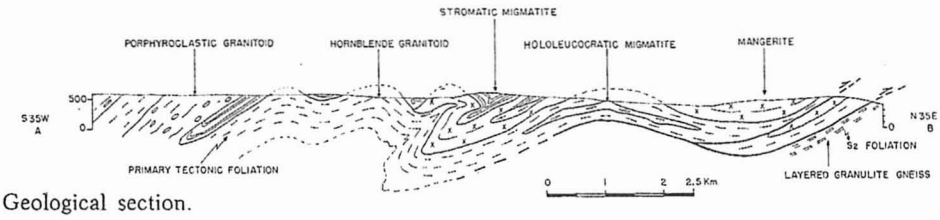

Figure 3 — Geological section.

deform the main foliation and re-orientate the isoclinal folds of the earlier phase towards EW. They are normal folds with weak axial dips, locally developing an axial plane cleavage.

These late folds correspond to two superposed folding phases: the NW-SE oriented folds are homoaxial to the isoclinal earlier folds developing interference figures of the type 3; the later NNE-SSW folds are discontinuous and have larger wavelenghts.

NE-SW oriented transcurrent faults with minor mylonitic-protomylonitic zones are associated to these late structures. Normal faults with the same direction seem to represent the terminal ruptile features.

THE SÃO JOSÉ DO RIO PARDO MANGERITIC-GRANITIC SUITE

Geology

The mangeritic-granitic rocks crop out in the São José do Rio Pardo region, as two parallel batholithic masses elongated NW-SE (Fig. 2).

The northernmost occurrence (São José do Rio Pardo massif) presents a very irregular shape, mainly due to a NE-SW refolding. It is tabular (minimum thickness of about 500 m), extending for about 60 km within the surrouding migmatitic gneisses; width is variable, generally between 2 and 3 km.

Pink, inequigranular coarse-grained, gneissic hornblende granites generally occupy the basal portions of the sheet, topped by strongly foliated mangerites, which are in some places replaced by pink granitoids (cf. Fig. 3); field work was not enough to determine if these pink varieties correspond to true hornblende granites or to hydrated "retrometamorphosed" mangerites.

No intrusive contacts were observed between hornblende granites and mangerites. In a few outcrops intermediate pale green rocks with a slight pink tint form a transitional passage between green "mangeritic" and pink "granitic" rocks.

A hornblende granite occurrence at the extreme SW corner (Fig. 2; N of Itobi) is separated from the São José do Rio Pardo massif by a band dominated by porphyroclastic granitoids, and continues, to the SE, with the São Roque da Fartura "charnockitic" massif (Morales, 1988); its total lenght is around 40 km, with widths around 2 km.

Another occurrence related to the suite (the São Pedro de Caldas massif) is situated to the E of the Cretaceous Poços de Caldas alkaline massif, extending for approximately 40 km in an E-W direction (Fig. 1). It is mainly formed by a succession (from "base" to "top") of hornblende granites, charnockites and mangerites, in which no intrusive or abrupt contacts are seen (V.A. Janasi, in prep.).

The contact relations between the mangeritic-granitic sheets and the surrounding rocks are to a great extent unknown. Contacts are almost always obscured by migmatisation; they are parallel to the strong foliation present in all lithologies.

The sheets are intrusive into the gneisses which constitute the mesosomes of the stromatic migmatites, as shown in sparse outcrops in the São Pedro de Caldas area (intrusive contacts, xenoliths) (V.A. Janasi, in prep.).

Contacts with the porphyroclastic granitoids were not observed. The intrusion of both plutonic associations preceded the main metamorphic-deformational event in the region; they do not show any evidence of a previous tectonic foliation. On the other hand, several arguments suggest that they are not contemporaneous: the mangerites-hornblende granites generated in an anorogenic environment (see below), while the porphyroclastic granitoids show features that are similar to those presented by calc-alkaline series typical of orogenic environments.

The pink nebulitic granites are associated with the late migmatisation, and are later than the mangeritic-granitic sheets, locally intruding them as thin dykes.

In some outcrops, the gneissic mangerites and hornblende granites are cut by isotropic "granitic" mobilizates that seem to have been gen-

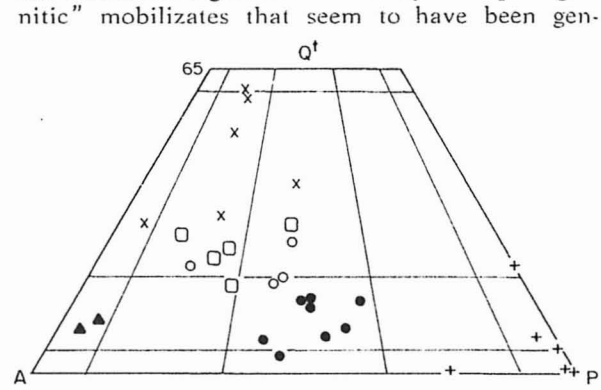

Figure 4 — São José do Rio Pardo lithologies plotted in the Streckeisen QAP modal diagram. Closed circles, mangerites; open cicles, hornblende granites; open squares, charnockites; X, hololeucocratic granites; closed triangles, syenitic rocks; +, enclaves.

erated by "in situ" anatexis in the axial planes of later folds.

Petrography

The mangerites are green coloured (from olive green to greyisch-green) medium to coarse grained rocks generally with a strong tectonic foliation with mineral stretching and flattening.

The available modal analyses classify most of them as quartz mangerites (Fig. 4) with quartz contents ranging from 5 to 17%. This variation can be in part attributed to the difficulty of performing precise modal analyses in such coarse-grained and foliated rocks. Their color index varies from 10 to 15.

The texture is seriate granoblastic with some alkali feldspar crystals slightly more prominent. Alkali feldspar is generally mesoperthitic and lacks cross-hatched twins, except for some of the smaller crystals and the borders of the larger ones. Plagioclase is oligoclase, ocasionally with antiperthitic exsolutions; the smaller crystals appear as agregates in mosaic textures. Quartz is flattened along the foliation. Clinopyroxene and hypersthene generally occur as separate grains but can also appear intimately associated when they occur as larger crystals; olive-green amphibole may appear at the borders of pyroxenes or as isolated grains. The common accessory minerals are zircon, opaques (mainly magnetite), apatite, and occasionally biotite, allanite and sphene. Products of retrogression of the pyroxenes are relatively frequent and besides the olive-green amphibole, colorless amphibole and brown biotite (rich in quartz inclusions) also occur.

Some rocks richer in alkali feldspar are locally found, specially in the northwestern part of the area of Figure 2. Modally (Fig. 4) they correspond to alkali feldspar-quartz syenitic rocks (quartz 10%) with either pyroxene or amphibole and with color index of about 15.

Rocks with charnockitic s.s. composition are relatively rare in the studied area, although they occur in nearby regions (Morales, 1988; V.A. Janasi, unpublished data). In the field they are conspicuous by the abundance of stretched quartz crystals and by a smaller color index compared with the mangerites.

In the studied area, green-colored, foliated fine grained charnockites appear in some outcrops as dyke-like restricted (decimetric) bands among the mangerites. Their quartz and alkali feldspar contents (Fig. 4) are always larger than those of the mangerites.

The hornblende granitoids strongly contrast with the mangerites by their pink colors and comparatively high (> 20%) quartz contents. They are coarse grained inequigranular and have a striped structure due to the alignment and stretching of the amphiboles along the tectonic foliation. A more intense deformation may generate an augen structure with large pink alkali feldspar crystals and well stretched quartz crystals. Their composition is granitic s.s. (Fig. 4) and they have color indices ranging from 4 to 9.

The mineralogy of the hornblende granite is somewhat similar to that of the mangerites with the exception of the absence of pyroxenes and predominance of olive-green amphibole with low 2V angle (Fe-hastingsite?) among the mafic minerals. Subordinately occurs brown biotite in part due to the retrogression of amphibole.

Hololeucocratic granites with color indices between 1 and 2 are relatively common among the hornblende granite outcrops, locally forming small bodies. They are medium to fine grained, have pronounced gneissic structure and are almost solely constituted by strongly perthitic pink alkali feldspar and discoid quartz, with a typical flaser texture. Their composition is granitic s.s. to alkali feldspar granitic, some terms being quartz-rich (Fig. 4). They correspond to the alaskitic granulites of Oliveira (1973).

Geochemistry

The chemical analyses for the samples with prefix CAN have been performed at the Department of Earth Sciences, Memorial University of Newfoundland (MUN). Major and minor elements were determined by AAS. while the trace elements were determined by XRF with estimates of analytical errors of about 5% or 1 ppm, whichever is greater.

The chemical analyses for the samples with prefix RP or G (Campos Neto & Figueiredo, 1985) were done by PURIQUIMA, with Rb, Sr, Ba, Zr, Nb and Y being determined by XRF, P_2O_5 by colorimetry and the other elements by AAS.

Chemical data for 30 whole-rock samples from the São José do Rio Pardo region is presented in Table 1, with sample location on Figure 5, showing a clear contrast between the mangerites (samples 1 to 14) and hornblende granites (samples 24 to 29). A comparison of the data from the two laboratories shows that the samples analysed at MUN have lower MnO and Ni content and a slightly better geochemical coherence. When there was a discrepancy in the data, the MUN results were considered as more reliable and selected to define typical compositions.

The mangerites, generally with SiO_2 contents ranging from 58 to 63%, have relatively high Al_2O_3 (16.5-18.3%), FeO_t (4.3-5.9%), Na_2O (4.3-5.3%) and K_2O (3.6-5.7%) contents and relatively low CaO (2.5-3.9%) and MgO (0.5-1.7%) contents, compared with typical intermediate rocks. Among the trace elements, high amounts of Ba (2100-3500 ppm), Zr (300-850 ppm), Nb, Y and Zn are conspicuous. Sr ranges from 300 to 600 ppm while Rb varies from 60

to 80 ppm. Three mangeritic samples (12, 13 and 14) have slightly higher SiO_2 contents (about 65%) and can be considered as "acid mangerites" in analogy to the classification adopted by Ormaasen (1977) for similar rocks in the Lofoten-Vesteraalen province in Norway. Compared with the more abundant "normal" mangerites they have less FeO_t (about 2.2%) and Zr (160-180

Table 1 — Chemical data from the São José do Rio Pardo Suite.

	Mangerites										
	1 G135	2 G22	3 CAN13C	4 CAN13B	5 CAN13E	6 G119	7 CAN13I	8 CAN13D	9 CAN13A	10 RP 174	11 RP 245
SiO_2	58.10	59.60	59.80	60.00	60.30	60.80	61.20	61.80	62.00	62.30	63.00
TiO_2	0.91	0.95	0.78	0.96	0.92	0.57	0.76	0.70	0.94	0.86	0.76
Al_2O_3	16.67	17.10	16.80	17.10	18.30	17.77	17.70	17.30	16.90	16.96	16.48
FeO_t	7.01	5.83	5.62	5.90	4.48	4.45	4.64	4.32	5.57	5.65	5.31
MnO	0.27	0.23	0.12	0.12	0.11	0.26	0.12	0.12	0.12	0.19	0.19
MgO	1.15	0.84	1.63	1.73	1.21	0.88	0.78	0.52	1.62	0.78	0.49
CaO	4.49	3.10	3.68	3.86	3.40	2.87	2.82	2.52	3.74	3.42	2.64
Na_2O	4.73	4.65	4.88	5.10	5.26	4.44	5.18	5.04	4.92	3.23	4.34
K_2O	3.61	5.25	4.32	3.76	4.55	5.68	4.91	5.52	4.20	4.87	4.93
P_2O_5	0.38	0.38	0.32	0.30	0.24	0.19	0.14	0.17	0.28	0.27	0.30
LOI			0.45	0.16	0.21		0.32	0.42	0.24		
Rb	54	61	83	61	64	78	73	75	70	75	82
Sr	610	600	405	446	468	455	356	299	400	443	330
Ba	2200	3500	2138	2285	3530	3200	2694	2634	2109	2400	2200
Zr	765	855	367	302	635	580	642	373	281	490	670
Nb	18	6	29	33	16	15	15	17	29	16	25
Y	32	18	51	49	29	15	29	24	50	20	27
Zn	56	60	56	48	51	46	56	48	52	36	59
Pb	19	23	17	21	16	17	16	13	22	15	22
Ni	18	18	2	n.d.	n.d.	11	n.d.	n.d.	n.d.	15	15
V	35	15	20	49	11	15	14	n.d.	38	15	10
Cr	6	5	8	8	5	3	4	6	8	4	7
Ga			21	23	16		19	25	19		
La			50	34	31		45	31	40		
Ce			96	104	75		79	69	98		
Th			12	5	8		2	9	19		
U			20	4	5		n.d.	n.d.	7		

	Mangerites			High-Fe mangerites				Basic enclaves		Syenites	
	12 CAN13F	13 CAN13H	14 RP 138	15 CAN13J	16 RP30F	17 RP48a	18 CAN13G	19 G 19b	20 G 46	21 G 131c	22 G 116b
SiO_2	64.00	64.40	65.60	57.30	58.80	59.70	60.50	49.80	50.20	60.10	64.20
TiO_2	0.16	0.22	0.65	1.24	1.39	0.66	0.88	1.03	1.15	1.01	0.80
Al_2O_3	17.80	17.40	17.68	15.10	14.35	14.48	15.70	13.41	14.70	14.75	13.67
FeO_t	2.23	2.21	2.78	10.61	8.12	8.42	7.79	5.52	3.76	5.50	4.59
MnO	0.04	0.03	0.09	0.29	0.26	0.35	0.22	0.49	0.30	0.14	0.12
MgO	0.58	0.54	0.59	1.00	1.51	0.58	0.65	6.51	7.85	2.00	1.50
CaO	2.38	2.20	1.71	3.86	3.66	4.18	3.20	8.47	8.07	3.32	2.66
Na_2O	4.80	4.62	3.06	4.33	4.42	4.63	4.36	3.03	2.51	2.30	2.18
K_2O	6.08	6.17	6.85	4.32	4.68	5.16	5.01	1.08	1.06	7.08	6.60
P_2O_5	0.12	0.13	0.13	0.45	0.63	0.24	0.26	0.19	0.47	0.88	0.74
LOI	0.51	0.50		0.12			0.71				
Rb	111	116	134	83	78	71	88	9	23	188	173
Sr	328	315	345	274	333	207	268	667	800	1600	1500
Ba	2502	2385	1100	2025	1800	1500	2114	450	850	5000	5000
Zr	162	181	550	685	570	1180	698	110	150	855	800
Nb	8	12	11	37	29	15	35	11	22	23	25
Y	35	34	41	56	41	33	47	26	16	47	41
Zn	22	19	25	99	81	84	62	180	76	37	48
Pb	27	23	24	22	21	21	24	25	14	17	19
Ni	n.d.	n.d.	23	n.d.	25	12	n.d.	70	180	32	25
V	5	5	15	n.d.	50	15	n.d.	300	155	45	30
Cr	8	6	4	10	13	13	8	22	320	28	14
Ga	21	22		21			17				
La	39	28		53			44				
Ce	91	99		80			52				
Th	14	14		9			6				
U	11	6		1			1				

Table 1 (cont.)

	Charnockite	Hornblende granitoids						Hololeucocratic granitoid
	23 G 86	24 RP 107c	25 CAN 8A	26 CAN 8B	27 RP 65	28 CAN 8c	29 RP 207b	30 RP 47
SiO_2	69.10	66.80	68.00	68.10	68.10	68.40	68.90	74.50
TiO_2	0.52	0.74	0.55	0.63	0.49	0.65	0.59	0.23
Al_2O_3	13.60	14.54	13.60	13.60	13.38	13.30	14.35	12.41
FeO_t	4.67	3.46	4.28	4.66	4.84	4.51	3.60	2.50
MnO	0.16	0.12	0.09	0.11	0.14	0.10	0.17	0.06
MgO	0.21	0.69	0.37	0.41	0.30	0.37	0.55	0.15
CaO	1.72	2.61	1.92	1.96	2.51	1.80	2.06	1.13
Na_2O	2.67	3.54	3.64	3.64	3.12	3.52	2.64	2.33
K_2O	5.47	5.07	5.65	5.38	5.97	5.34	5.69	5.45
P_2O_5	0.11	0.22	0.12	0.13	0.08	0.12	0.13	0.02
LOI			0.27	0.14		0.33		
Rb	86	170	151	150	126	151	117	143
Sr	115	220	137	137	184	130	285	93
Ba	900	870	899	949	1000	880	1800	530
Zr	650	380	561	609	550	596	525	330
Nb	12	31	48	45	14	49	17	10
Y	23	51	93	99	51	95	31	54
Zn	72	46	83	89	60	91	37	28
Pb	17	23	30	20	23	32	15	19
Ni	18	20	4	5	5	5	10	8
V	10	10	n.d.	n.d.	10	n.d.	10	5
Cr	17	10	1	n.d.	24	7	11	27
Ga			20	19		22		
La			111	109		124		
Ce			161	185		184		
Th			13	18		20		
U			n.d.	n.d.		7		

n.d., not detected

ppm) and more K_2O (about 6%).

Another subordinate group (samples 15-18, Table 1) has somewhat different geochemical characteristics, compared with the "normal" mangerites, having higher $Fe_t/(Fe_t + Mg)$ (F/FM) indices (due to their high FeO_t contents 7.8-10.6%), lower Al_2O_3 (14.4-15.7%), Ba (1500-2100 ppm) and Sr (200-300 ppm), and slightly higher Zn (60-100 ppm), corresponding to high Fe mangerites.

The syenitic rocks (samples 21 and 22, Table 1) have F/FM indices lower than those from the "normal" mangerites and other distinct characteristics such as higher K_2O (6.6-7.1%), Rb (about 180 ppm), Sr (1500 ppm), Ba (5000 ppm), Zr (800-850 ppm) and P_2O_5 (0.8%) and lower Na_2O (about 2.2%) contents.

The hornblende granites (samples 24-29, Table 1) have SiO_2 values ranging from 66.8 to 68.9%. Compared with the mangerites they have lower Al_2O_3 (13.3-14.5%) and Na_2O (3.1-3.6%). Their FeO_t (3.5-4.8%) and K_2O (5.1-6.0%) contents are relatively high and CaO (1.8-2.6%) and MgO (0.3-0.7%) are relatively low for this SiO_2 interval. Ba ranges from 870 to 1000 ppm, Sr from 130 to 220 ppm, and Rb from 130 to 170 ppm. The HFS elements (Zr, Nb and Y) are quite abundant.

Just one sample (30, Table 1) of hololeucocratic granite was analysed and it appears to correspond to a more differentiated term of the hornblende granites, also having relatively high F/FM and K_2O and low CaO. One sample (23, Table 1) corresponds to a fine grained charnockite, having chemical characteristics similar to those from the hornblende granites. Basic enclaves occur subordinately in the mangerites and two samples (19 and 20, Table 1) have been analysed and may be classified as norite.

Variation diagrams (Fig. 6) for the São José do Rio Pardo lithologies clearly show the distinction between the mangerites and hornblende granites, particularly in Al_2O_3 and Na_2O. The basic enclaves have MgO, K_2O and Al_2O_3 contents quite different from those of the mangerites, while there is a clear distinction in terms of Na_2O and MgO for the syenitic rocks.

The São José do Rio Pardo rocks cluster towards the alkali apex of the AFM diagram (Fig. 7), like other similar suites such as the Hopen mangerite-charnockite intrusion of northern Norway (Ormaasen, 1977).

In the R1-R2 diagram (De La Roche *et al.*, 1980) the mangerites plot on the syenite-quartz syenite-quartz monzonite fields, the hornblende granites plot on the monzogranite and syenogranite fields, and the basic enclaves on the olivine gabbro field (Fig. 8). The main trend of the mangerites and hornblende granites is similar to that of late orogenic granitoids (Batchelor & Bowden, 1985).

In the calc-alkali ratio versus SiO_2 diagram

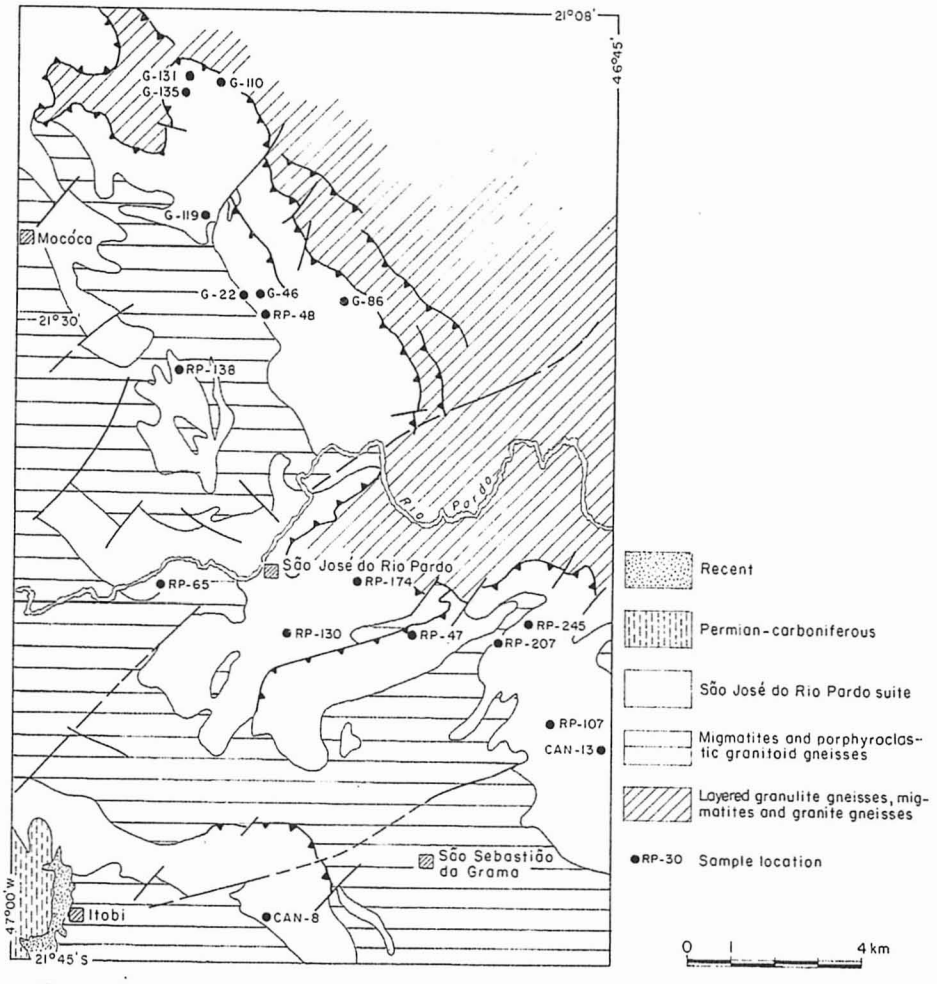

Figure 5 — Simplified geological map of the São José do Rio Pardo region with sample location.

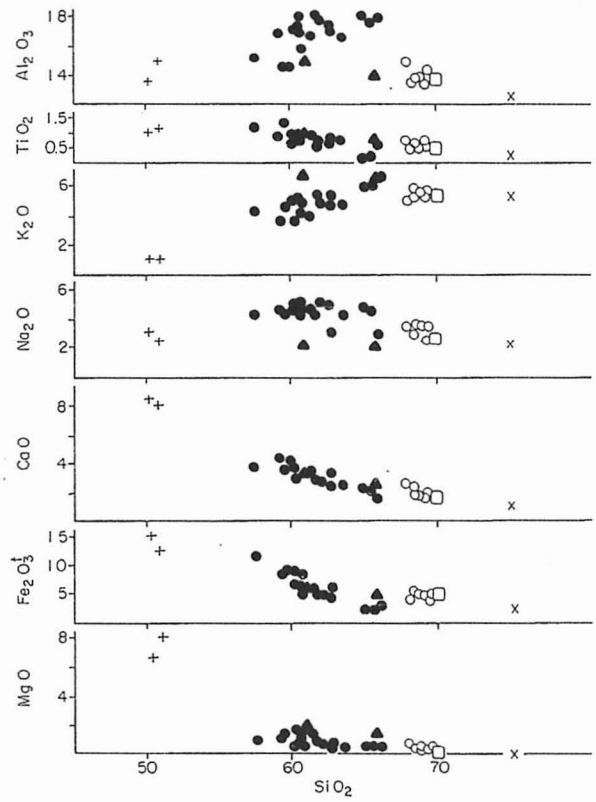

Figure 6 — São José do Rio Pardo lithologies plotted in the Harker diagrams. Simbology as Fig. 4.

(Fig. 9) the mangerites and hornblende granites plot mainly on the alkali-calcic to alkaline field but due to their relatively small silica range it is not possible to determine precisely their alkali-lime index (Peacock, 1931). The mangerites plot very near the trend of the Hopen intrusion (after Ormaasen, 1977), while the hornblende granites appear to have slightly larger calc-alkali ratios.

The Rb versus Nb + Y diagram (Fig. 10) suggests that the mangerites and hornblende granites are comparable to post-collisional and within

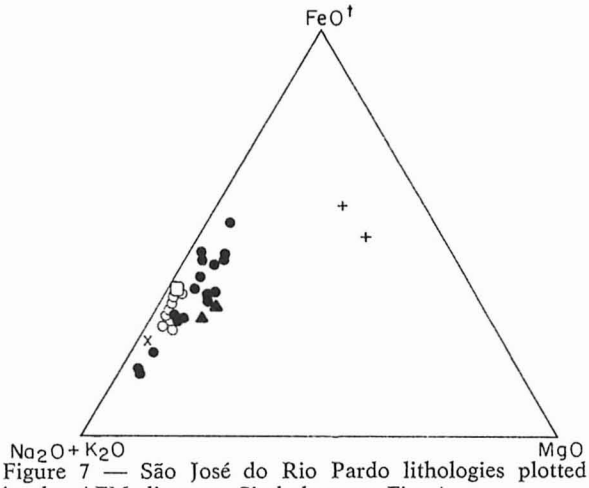

Figure 7 — São José do Rio Pardo lithologies plotted in the AFM diagram. Simbology as Fig. 4.

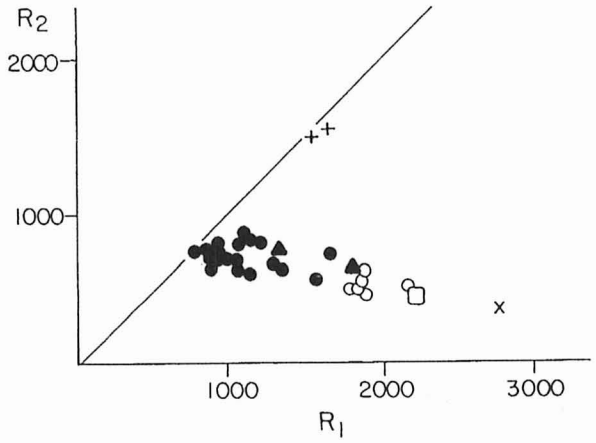

Figure 8 — São José do Rio Pardo lithologies plotted in the R1-R2 diagram (De La Roche *et al.*, 1980). Simbology as Fig. 4.

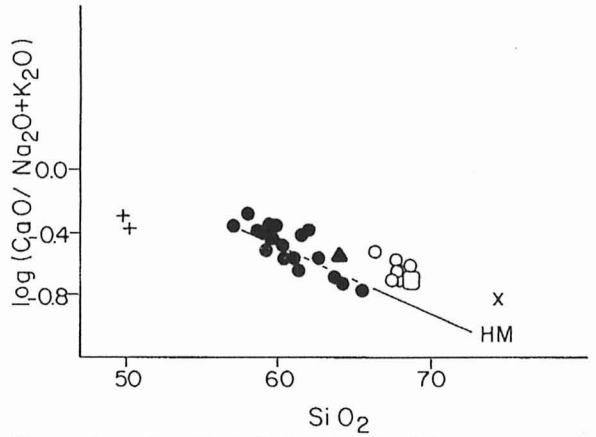

Figure 9 — São José do Rio Pardo lithologies plotted in the calc-alkali ratio versus silica diagram (Brown, 1982). Simbology as Fig. 4; HM, trend of the Hopen mangerite-charnockites (after Ormaasen, 1977).

plate granitoids (Pearce *et al.*, 1984).

In the Rb-Sr (Fig. 11) and Rb-Ba (Fig. 12) diagrams the mangerites and hornblende granites fall on a same trend of decreasing Sr and Ba with increasing Rb. The syenitic rocks are considerably enriched in Sr and Ba, while the charnockite, basic enclaves and the hololeucocratic granite are poorer in Sr and Ba, compared with the mangerites and hornblende granites.

The La-Ce-Y normalized distribution (Fig. 13) shows that the hornblende granites have higher contents of these elements in relation to the mangerites, but with similar Ce/Y_N ratios (about 4). Considering Y as representative of the heavy rare earth elements, the patterns observed for the São José do Rio Pardo rocks are similar to the REE patterns for mangeritic rocks from Lofoten-Vesteraalen (Green *et al.*, 1972; Ormaasen, 1977).

A compositional comparison of the São José do Rio Pardo mangerites and hornblende granites with similar occurrences, typical of the Middle Proterozoic anorogenic plutonism in several regions of the northern hemisphere, is presented on Tables 2 and 3.

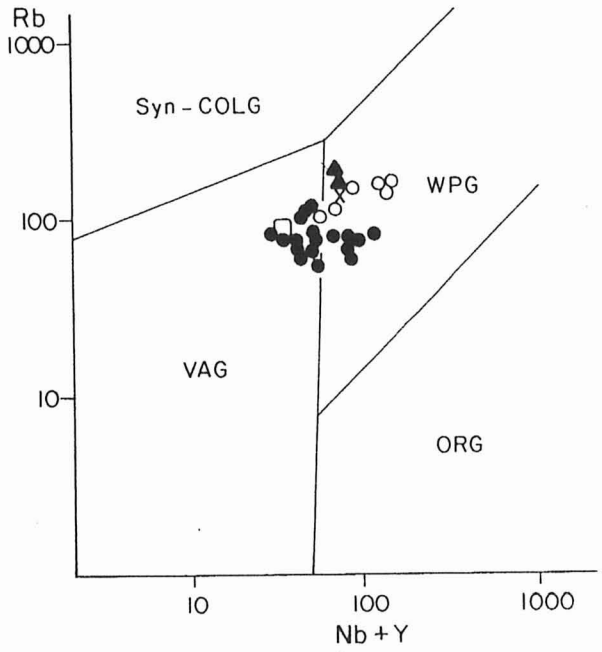

Figure 10 — São José do Rio Pardo lithologies plotted in the Rb versus Nb+Y diagram (Pearce *et al.*, 1984). Simbology as Fig. 4; syn-colg, field of syn-collisional granitoids; WPG, field of within plate granitoids; VAG, field of volcanic arc granitoids; ORG, field of ocean ridge granitoids.

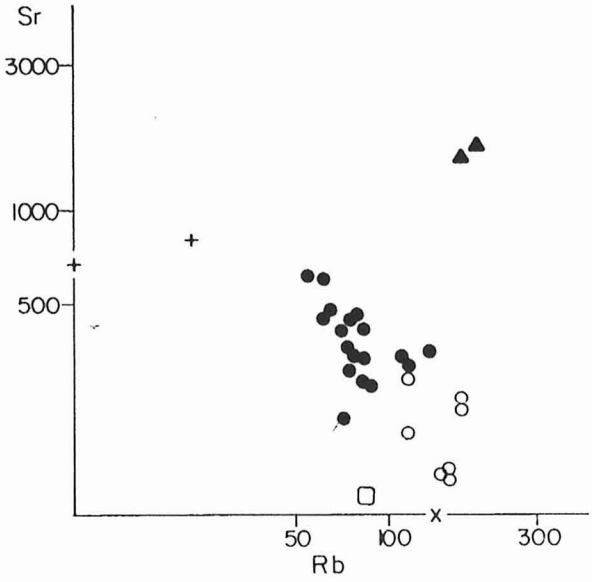

Figure 11 — São José do Rio Pardo lithologies plotted in the Rb-Sr diagram. Simbology as Fig. 4.

The São José do Rio Pardo mangerites can be separated into "normal" mangerites and less abundant high-Fe mangerites, as also occurs in the Lofoten-Vesteraalen massif (Ormaasen, 1977). The "normal" mangerites are quite similar to the Lofoten mangerites with lower F/FM ratios (less than 0.8), such as the southwestern Lofoten massif (Ormaasen, 1977). On the other hand, the high-Fe mangerites resemble the Lofoten-Raftsund massif (Griffin *et al.*, 1974) and the "adamellites" (fayalite-clinopyroxene granitoids) with the same SiO_2 range which occur bordering

Table 2 — Chemical comparison between São José do Rio Pardo mangerites and similar occurrences. F/FM, $(Fe_t/(Fe_t + Mg)$ (mol. prop.); ALC, $Na_2O + K_2O$ (1) Typical São José do Rio Pardo mangerites (average of analyses 3, 4, 5, 7, 8 and 9, Table 1); (2) High-Fe São José do Rio Pardo mangerites (average of analyses 15 to 18, Table 1); (3) Average mangerite, SW Lofoten massif, Lofoten-Vesteralen, Norway (Ormaasen, 1977); (4) Average high-Fe mangerite Raftsund massif, Lofoten-Vestaralen, Norway (Griffin *et al.*, 1974; Ormaasen, 1977); (5) Harp Lake "adamellites" Canada (average of 5 analyses extracted from Emslie, 1980).

	(1) Mangerite SJRP	(2) High-Fe Mangerite	(3) Norway SW Lofoten	(4) Norway Raftsund	(5) Canada Harp Lake
SiO_2	60.85	59.08	59.6	58.1	60.5
TiO_2	0.84	1.04	1.2	1.1	0.90
Al_2O_3	17.35	14.91	17.5	16.7	16.1
FeO_t	5.66	8.74	5.9	8.3	7.1
MnO	0.12	0.28	0.1	0.2	0.13
MgO	1.25	0.94	1.4	0.7	0.80
CaO	3.34	3.73	3.6	3.4	3.97
Na_2O	5.06	4.44	5.0	4.8	4.2
K_2O	4.59	4.79	5.1	5.3	4.67
P_2O_5	0.24	0.40	0.5	0.2	0.46
Total	99.30	98.35	99.9	98.8	98.83
F/FM	0.72	0.84	0.70	0.87	0.83
ALC	9.65	9.23	10.1	10.1	8.87

the Harp Lake anorthosite complex in Canada (Emslie, 1980).

The São José do Rio Pardo hornblende granites are compositionally quite similar to the wiborgitic-textured "rapakivi" granites from the type area (Wiborg massif, Finland, Simonen & Vorma, 1969). They are also similar to the biotite-hornblende granites of the Wolf River batholith in Wisconsin, USA (Anderson, 1983) and the Harp Lake "adamellites" (Emslie, 1980) with same silica range, but having slightly higher F/FM ratios.

The São José do Rio Pardo hololeucocratic granite is chemically comparable to other differentiated granites from several anorogenic provinces, such as the equigranular "rapakivi" granites from the Wiborg massif (Simonen & Vorma, 1969), and to biotite granites from the Wolf River and Pikes Peak batholiths (Anderson, 1983).

Geochronology

The isotopic analyses presented in Table 4 have been determined at the Department of Earth Sciences, Memorial University of Newfoundland. Strontium was isolated by conventional cation

Table 3 — Chemical comparison between São José do Rio Pardo granites and similar occurrences. (1) Typical São José do Rio Pardo hornblende granites (average of analyses 22, 23 and 25, Table 1); (2) Typical wiborgite, Wiborg massif, Finland (Simonen & Vorma, 1969); (3) Harp Lake "adamellites", Canada (average of 7 analyses extracted from Emslie, 1980); (4) Biotite-hornblende granite, Wolf River batholith, USA (average of 6 analyses, Anderson, 1983); (5) Hololeucocratic São José do Rio Pardo granite (analyses 27, Table 1); (6) "Equigranular Rapakivi", Wiborg massif (Simonen & Vorma, 1969); (7) Belongia granite, Wolf River batholith (average of 3 analyses, Anderson, 1983); (8) Biotite granite, Pikes Peak batholith, USA (average of 19 analyses, Anderson, 1983).

	(1) Hb-Gra SJRP	(2) Wiborgite Finland	(3) Harp Lake Canada	(4) Wolf River USA	(5) Holo Gra SJRP	(6) EQRAP Finland	(7) Wolf River USA	(8) Pikes Peak USA
SiO_2	68.17	68.88	68.46	68.22	74.50	74.87	75.73	72.59
TiO_2	0.61	0.49	0.70	0.56	0.20	0.23	0.19	0.28
Al_2O_3	13.50	13.74	14.16	14.87	12.41	12.39	12.21	13.36
FeO_t	4.48	4.54	5.58	4.36	2.50	2.12	2.06	2.50
MnO	0.10	0.06	0.09	0.09	0.06	0.02	0.04	0.07
MgO	0.38	0.47	0.30	0.45	0.15	0.24	0.13	0.14
CaO	1.89	1.92	2.12	1.94	1.13	0.82	0.70	1.18
Na_2O	3.60	2.94	3.3	3.59	2.33	2.42	2.92	3.31
K_2O	5.46	5.79	4.88	5.48	5.45	5.79	5.22	5.60
P_2O_5	0.25	0.14	0.13	0.14	0.02	0.03		
Total	98.44	98.97	99.72	99.70	98.75	98.93	99.20	99.03
F/FM	0.87	0.84	0.91	0.85	0.90	0.83	0.90	0.91
ALC	9.06	8.73	8.18	9.07	7.78	8.21	8.14	8.91

Table 4 — Sr and Rb isotopic data.

	Rb	Sr	Rb/Sr	$^{87}Rb/^{86}Sr$	$^{87}Sr/^{86}Sr$
CAN 13A	72.3	402.1	0.1798	0.52070	0.71373
CAN 13B	66.0	439.2	0.1502	0.43491	0.71258
CAN 13C	78.8	410.4	0.19198	0.55617	0.71382
CAN 13D	74.3	304.0	0.2443	0.70766	0.71673
CAN 13F	115.3	330.9	0.3487	1.0102	0.71880
CAN 13G	85.3	268.0	0.3185	0.92284	0.71855
CAN 13H	114.4	320.7	0.3568	1.0338	0.71891
CAN 13I	74.3	356.4	0.2084	0.60355	0.71450
CAN 13J	75.4	275.0	0.2740	0.79388	0.71740
CAN 15A	158.7	195.3	0.8127	2.3586	0.73516
CAN 15B	153.1	178.4	0.8586	2.4925	0.73814
CAN 15C	189.3	261.4	0.7240	2.1003	0.72955
CAN 15D	148.2	224.7	0.6595	1.9124	0.72681
CAN 15E	130.9	305.9	0.4279	1.2402	0.72074
CAN 15F	83.5	195.6	0.4267	1.2368	0.72215
CAN 15G	97.3	442.0	0.2202	0.63775	0.71378
CAN 15H	89.9	415.6	0.2175	0.62980	0.71370

exchange methods and analyzed isotopically using a Micromass 30B thermal ionization mass spectrometer with a Faraday collector. Data acquisition and reduction was controlled by an on-line Hewlett-Packard HP-85 desktop computer. Rubidium and strontium concentrations were determined by XRF based on a minimum of ten replicate analyses and calibrated against international rock standards. Precision of Rb and Sr concentrations is estimated at about 5% or 0.3 ppm, whichever is greater. Initial Sr isotopic compositions were calculated using a ^{87}Rb decay constant of 1.42 E-11/year.

Previously available Rb/Sr isotope data for mangeritic-charnockitic rocks from the São José do Rio Pardo region (Oliveira *et al.*, 1986) yielded Late Proterozoic ages. Whole-rock isochrons indicated 650 ± 40 and 660 ± 125 Ma, with $^{87}Sr/^{86}Sr$ initial ratios of 0.7078 and 0.7093, respectively.

Both these previously available data and the new Rb/Sr isotope data presented in Table 4 indicate isotopic incomplete homogenization probably due to the complex evolution shown by field, petrographic and structural data. Therefore, we have used mixing diagrams (Faure, 1986), where the analytical points are plotted in a diagram with $^{87}Sr/^{86}Sr$ ratios versus the reciprocals of the strontium concentrations, to select which samples should be used for isochron calculation.

Using the data from Oliveira *et al.* (1986), only a few points plot on a straight line (Fig. 14a) some of these points are from a single outcrop (JD 184) and define the isochron with 650 ± 40 Ma cited above. The other samples which also plot on the same line in Figure 14a aligned in a straight line correlative to an isochron of about 1270 ± 180 Ma with $^{87}Sr/^{86}Sr$ initial ratio of 0.7048 (Fig. 14b), although they came from different outcrops.

The Rb/Sr data for the mangerite CAN 13 outcrop (Table 4), when plotted in the mixing diagram (Fig. 15a) show that only two samples

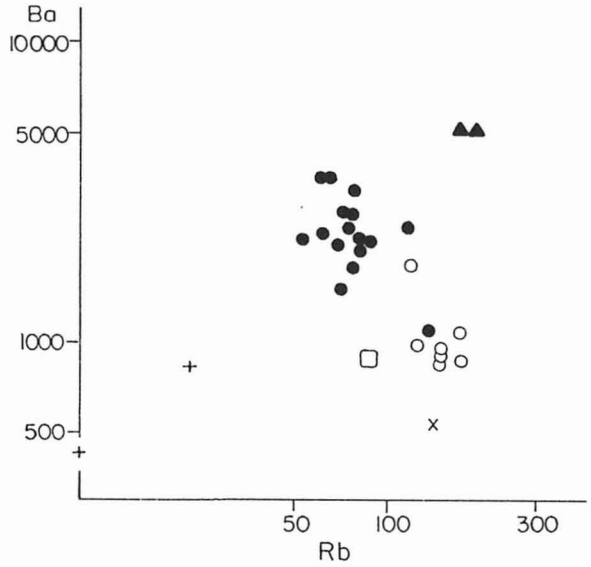

Figure 12 — São José do Rio Pardo lithologies plotted in the Rb-Ba diagram. Simbology as Fig. 4.

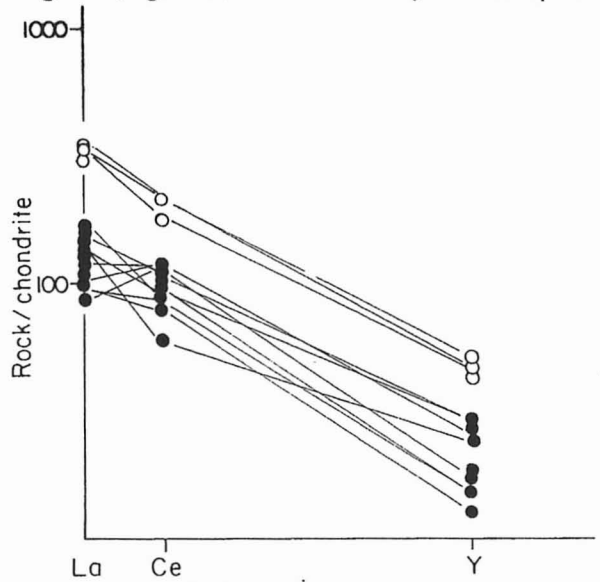

Figure 13 — São José do Rio Pardo mangerites (closed circles) and hornblende granites (open circles) plotted in the chondrite-normalized La-Ce-Y diagram.

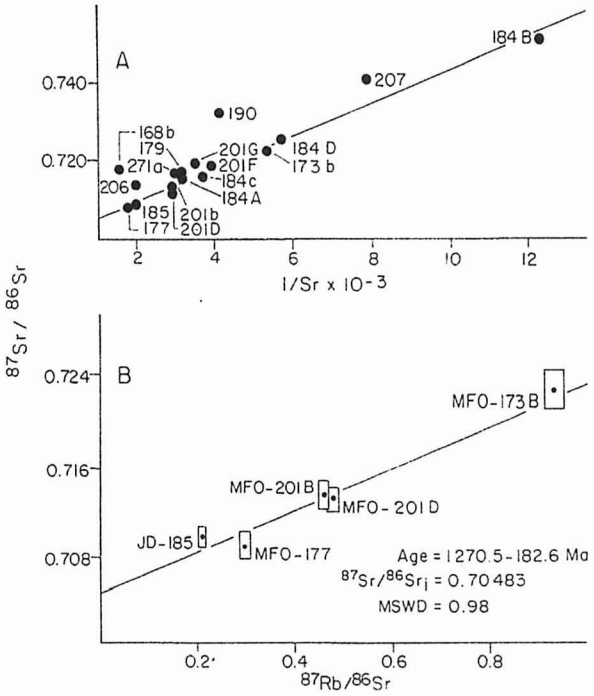

Figure 14 — Rb-Sr data for São José do Rio Pardo mangeritic rocks (Oliveira *et al.*, 1986). A. Mixing diagram; B. Rb-Sr reference isochron.

(CAN 13f and CAN 13h) do not have a good fitting in a straight line. The other samples define a single outcrop isochron with an age of about 930 ± 16 Ma with $^{87}Sr/^{86}Sr$ initial ratio of 0.7067 (Fig. 15b).

The Rb/Sr isotope data for the pink migmatite CAN 15 outcrop (Table 4), located at 46°39' W and 21°35' S coordinates, when plotted in the mixing diagram (Fig. 16a) suggest that five of the samples, including pink granitic leucosomes and dark grey gneissic mesosomes, could be used for constructing an isochron, yielding and age of about 830 ± 8 Ma with R_o of 0.7057 (Fig. 16b).

Results of U-Pb age determinations in two samples of clearly zoned zircons (Oliveira *et al.*, 1986) defined a poorly precise upper intercept

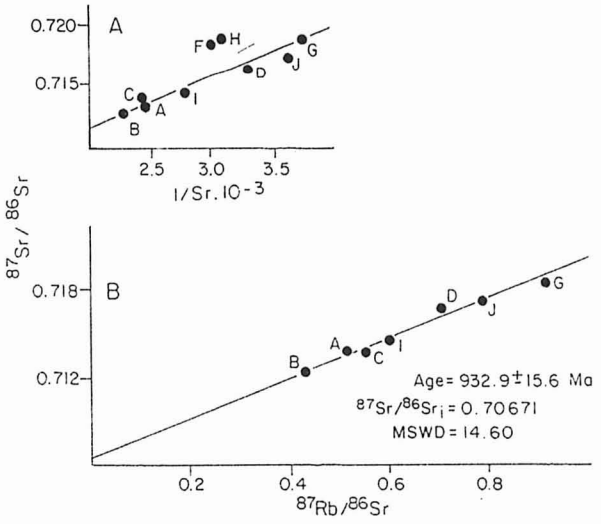

Figure 15 — Rb-Sr data for the CAN 13 mangeritic outcrop. A. Mixing diagram; E. Rb-Sr isochron.

of 780 Ma in a Concordia plot. K-Ar determinations (Oliveira, 1973) indicate an important thermal event at about 600 Ma.

The existing data is interpreted as follows. The Rb/Sr ages of 930 and 830 Ma obtained in this work seems to delimit the interval of the main metamorphic event (accompanied by profuse anatexis) and the development of the tectonic foliation in the mangerites. Younger Rb/Sr ages around 650 Ma overlaps with K/Ar amphibole data, and are attributed to local isotopic rehomogenization associated with later events of deformation and metamorphism imprinted in these rocks. Based on geological arguments (see below), we suggest that the Rb/Sr alignment around 1300 Ma (Fig. 14b) may approximate the intrusion age of the São José do Rio Pardo suite.

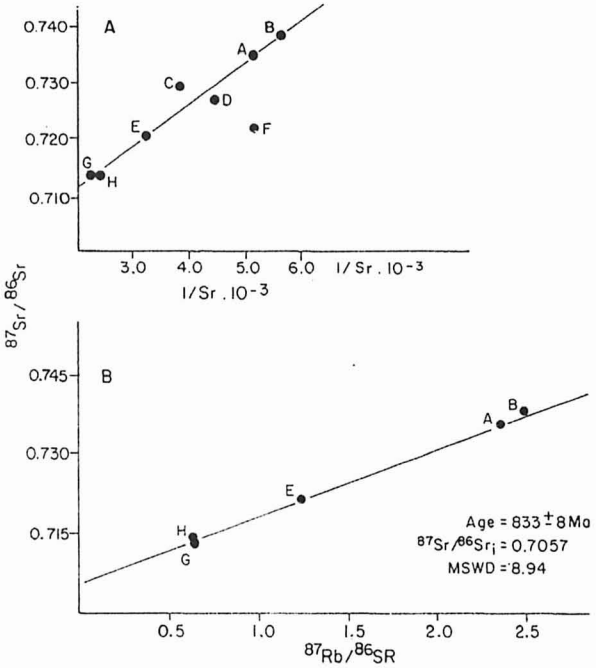

Figure 16 — Rb-Sr data for the CAN 15 pink migmatitic outcrop. A. Mixing diagram; B. Rb-Sr isochron.

CONCLUSIONS

The mangerites and hornblende granites of the São José do Rio Pardo suite show an intimate relation, forming tabular bodies up to several hundred meters thick. The hornblende granites usually occur in the basal portions of the sheets, suggesting an inverse position relative to the normal differentiation sequence.

Charnockitic and syenitic compositions are subordinate in the studied area. Noritic and amphibolitic enclaves are scarcely found and do not appear to have a direct genetic link with the suite.

All the lithologies present in the suite are gneissic, with a refolded tectonic foliation, except for local "granitic" veins formed by subsequent anatexis. Igneous textures are almost totally destroyed.

Geochemically, the suite is characterized by

rocks of relatively high contents of Fe/(Fe + Mg), K and HFS elements and low Ca, and are quite similar to typical Middle Proterozoic anorogenic mangerites and rapakivi granites found elsewhere.

The Rb/Sr isotope data show incomplete isotopic homogenization attributed to the complex geologic evolution of the region. The mangerites yielded and age of about 930 Ma with R_o of 0.7067, considered to be near the main metamorphic event. Some features, such as the anorogenic character of the suite, its Late Proterozoic metamorphism and deformation, and the existence of an important Middle Proterozoic orogenic event on a regional scale (which was not imprinted in these rocks) suggest to us that the age of about 1300 Ma could approximately represent the intrusive episode.

REFERENCES

ANDERSON, J.L. (1983) Proterozoic anorogenic granite plutonism of North America. Geol. Soc. Am., Mem. **161**:133-154.

BATCHELOR, R.A. & BOWDEN, P. (1985) Petrogenetic interpretation of granitoid rock series using multicationic parameters. Chem. Geol., **48**:43-55.

BROWN, G.C. (1982) Calc-alkaline intrusive rocks: their diversity, evolution and relation to volcanic arcs. In: R.S. Thorpe (ed.) Andesites. Ed. John Wiley and Sons, p. 437-461.

CAMPOS NETO, M.C. & FIGUEIREDO, M.C.H. (1985) Geologia das Folhas São José do Rio Pardo e Guaranésia (porção paulista) 1:50.000. IG-USP, PRÓ-MINÉRIO, São Paulo, vol. 1, Geol. 123p.

CAMPOS NETO, M.C. (1985) Evolução do Pré-Cambriano paulista e regiões adjacentes. In: 5.° Simp. Reg. Geol., Rio Claro, Atas, **2**:561-571.

CAVALCANTE, J.C.; CUNHA, H.C.S.; CHIEREGATI, L.A.; KAEFER, L.Q.; ROCHA, J.M.; DAITX, E. C.; RAMALHO, R. (1979) Projeto Sapucaí. MME, DNPM, Sér. Geol. 4, Seção Geol. básica 2, Brasília, 299p.

DE LA ROCHE, H.; LETERRIER, J.; GRANDCLAUD, P.; MARCHAL, M. (1980) A classification of volcanic and plutonic rocks using R1-R2 diagrams and major elements analyses — its relationships with current nomenclature. Chem. Geol., **29**: 183-210.

EBERT, H. (1968) Ocorrências da fácies granulítica no sul de Minas Gerais e em áreas adjacentes, em dependência da estrutura orogênica: hipóteses sobre sua origem. An. Acad. bras. Ciênc., **40**:215-229.

EMSLIE, R.F. (1980) Geology and petrology of the Harpe Lake Complex, central Labrador: an example of Elsonian magmatism. Geol. Surv. Canada, Mem., **293**, 136p.

FAURE, G. (1986) Principles of isotope geology. John Wiley & Sons, 589p.

GREEN, T.H.; BRUNFELT, A.I.; HEIER, K.S. (1972) Rare earth element distribution and K/Rb ratios in granulites, mangerites and anorthosites, Lofoten-Vesteraalen, Norway. Geochim. Cosmochim. Acta, **36**: 241-257.

GRIFFIN, W.L.; HEIER, K.S.; TAYLOR, P.N.; WEIGAND, P.W. (1974) General geology, age and chemistry of the raftsund mangerite intrusion, Lofoten-Vesteraalen. Norges Geol. Unders., **312**:1-30.

HASUI, Y. & OLIVEIRA, M.A.F. (1984) Província Mantiqueira setor central. In: F.F.M. Almeida e Y. Hasui (coords.). O Pré-Cambriano no Brasil. Edgard Blücher Ltda., p. 308-344.

JOHANNES, W. & GUPTA, L.N. (1982) Origin and evolution of migmatite. Contrib. Mineral. Petrol., **79**:114-123.

MORALES, N. (1988) Evolução lito-estrutural das rochas pré-cambrianas da região de São José da Boa Vista. Dissertação de Mestrado. Instituto de Geociências, Universidade de São Paulo, 157p. [unpublished].

OLIVEIRA, M.A.F. (1973) Petrologia das rochas metamórficas da região de São José do Rio Pardo, SP. Rev. Bras. Geoc., **3**(4):257-278.

OLIVEIRA, M.A.F. & ALVES, F.R. (1974) Geologia e petrografia da região de Caconde, SP. In: 28.° Congr. Bras. Geol., Porto Alegre, Anais, **5**:133-143.

OLIVEIRA, M.A.F.; FRANCESCONI, R.; CORDEIRO, C.M.; INGLEZ, A.G.; OLIVEIRA, E.G.; SENA, C.A.S. (1983) Geologia da porção paulista das quadrículas Caconde e Guaxupé. In: 1.ª Jorn. Carta Geol. Est. S.P. em 1:50.000, São Paulo, PRÓ-MINÉRIO, p. 171-191.

OLIVEIRA, M.A.F.; MORALES, N.; FULFARO, V.J. (1984) Projeto Boa Vista. Rel. Final Conv. PRÓ-MINÉRIO-UNESP, vol. 1, 85p.

OLIVEIRA, M.A.F.; KAWASHITA, K.; KIHARA, Y.; DELHAL, J. (1986) Novos dados geocronológicos para rochas charnoquíticas da associação Guaxupé, Complexo Varginha. Rev. Bras. Geoc., **13**(13):301-305.

ORMAASEN, D.E. (1977) Petrology of the Hopen mangerite-charnockite intrusion, Lofoten, north Norway. Lithos, **10**:291-310.

PEACOCK, M.A. (1931) Classification of igneous rock series. J. Geol., **39**:54-67.

PEARCE, J.A.; HARRIS, N.B.W.; TINDLE; A.G. (1984) Trace element discrimination diagrams for the tectonic interpretation of granitic rocks. J. Petrol., **25**(4):956-983.

SIMONEN, A. & VORMA, A. (1969) Amphibole and biotite from rapakivi. Bull. Comm. Geol. Finlande, **238**, 28p.

TROUW, R.A.J.; RIBEIRO, A.E.; PACIULLO, F.V.P. (1983) Geologia estrutural dos Grupos São João Del Rei, Carrancas e Andrelândia, sul de Minas Gerais. Anais Acad. bras. Ciênc., **55**(1):71-85.

VASCONCELLOS, A.C.B.C. (1988) O Grupo Andrelândia na região de Ouro Fino, MG. Dissertação de Mestrado, Instituto de Geociências, Universidade de São Paulo, 199p. [unpublished].